Characterization of an AC glow-type gliding arc discharge in atmospheric air with a current-voltage lumped model

Kong, Chengdong; Gao, Jinlong; Zhu, Jiajian; Ehn, Andreas; Aldén, Marcus; Li, Zhongshan

Published in:
Physics of Plasmas

DOI:
10.1063/1.4986296

2017

Document Version:
Publisher's PDF, also known as Version of record

Physics of Plasmas

Characterization of an AC glow-type gliding arc discharge in atmospheric air with a current-voltage lumped model

Cite as: Phys. Plasmas **24**, 093515 (2017); https://doi.org/10.1063/1.4986296
Submitted: 03 June 2017 • Accepted: 23 August 2017 • Published Online: 08 September 2017

Chengdong Kong, Jinlong Gao, Jiajian Zhu, et al.

Characterization of an AC glow-type gliding arc discharge in atmospheric air with a current-voltage lumped model

Chengdong Kong,[1] Jinlong Gao,[1] Jiajian Zhu,[1,2] Andreas Ehn,[1] Marcus Aldén,[1] and Zhongshan Li[1]
[1]*Division of Combustion Physics, Lund University, P.O. Box 118, S-221 00 Lund, Sweden*
[2]*Science and Technology on Scramjet Laboratory, National University of Defense Technology, Changsha 410073, China*

(Received 3 June 2017; accepted 23 August 2017; published online 8 September 2017)

Quantitative characterization of a high-power glow-mode gliding arc (GM-GA) discharge operated in open air is performed using a current-voltage lumped model that is built from the perspective of energy balance and electron conservation. The GM-GA discharge is powered by a 35 kHz alternating current power supply. Instantaneous images of the discharge volume are recorded using a high-speed camera at a frame rate of 50 kHz, synchronized with the simultaneously recorded current and voltage waveforms. Detailed analyzation indicates that the electrical input power is dissipated mainly through the transport of vibrationally excited nitrogen and other active radicals (such as O). The plasma is quite non-thermal with the ratio of vibrational and translational temperatures (T_v/T_g) larger than 2 due to the intense energy dissipation. The electron number density reaches 3×10^{19} m^{-3} and is always above the steady value owing to the short cutting events, which can recover the electron density to a relatively large value and limits the maximum length of the gliding arc. The slow decaying rate of electrons is probably attributed to the decomposed state of a hot gaseous mixture and the related associative ionization. *Published by AIP Publishing.* [http://dx.doi.org/10.1063/1.4986296]

I. INTRODUCTION

Electrically generated plasmas have been commonly classified into two types: thermal and non-thermal plasmas. Thermal plasmas are typically hot and lack chemical selectivity, whereas non-thermal plasmas have much higher average electron energies in comparison to gas molecules and therefore are more chemically selective.[1] Owing to the chemical selectivity, non-thermal plasmas could be utilized in various applications such as combustion enhancement,[2,3] material treatment,[4–6] and gas conversion and decontamination.[7–10] Non-thermal plasmas can be produced by different techniques such as corona, dielectric barrier discharge (DBD), and gliding arc discharge. Among them, the gliding arc has been proved to provide a high operating power in non-thermal conditions at atmospheric pressure.[11]

Gliding arc discharge was intensively studied through experiments[12–14] and simulations.[15–18] Fridman and his coworkers from Drexel University[1–3,10,19–21] conducted a lot of pioneering work. Their results indicated that an arc discharge initiates at the smallest gap between two divergent electrodes and elongates with flow until extinction. The initial arc is hot, but due to the strong transverse gas flow, it elongates and cools down. During the elongation process, the arc requires more power from the power supply for self-sustaining. When a critical length corresponding to the maximal limit of power supply is reached, the gliding arc will "overshoot" this critical point a little before extinction. Then, a new gliding arc is initiated at the shortest gap and elongates until extinction. The process repeats in a cyclic manner at relatively high frequencies (100–500 Hz).[1] This physical picture indicates that the conventional gliding arc is unstable and experiences the transition from thermal to non-thermal states with frequent reignition and extinction. However, under certain conditions with a regulated gas flow rate and electrical input power, the gliding arc discharge has been found to sustain on a non-thermal state for a relatively long time without frequent extinction.[11] The radical profiles, the current/voltage characteristics, and the flow effect were analyzed on this special gliding arc.[22–26] Nevertheless, some fundamental questions are not well understood yet such as why the glow-mode gliding arc (GM-GA) can be sustained for a long time, how the input energy is dissipated, and how the non-equilibrium plasma is established.

With these questions, this article aims to explore the underlying physical mechanisms in the glow-mode gliding arc (GM-GA) based upon detailed diagnostics and modeling. The characteristics of the glow-mode gliding arc are first presented. Then, the sustaining mechanism is analyzed from the perspective of electron conservation and energy balance with a current-voltage lumped model. The effect of short-cutting events is emphasized to demonstrate the uniqueness of our gliding arc system in comparison to the conventional one.

II. METHODOLOGY

A. Experimental method

The details of the gliding arc discharge system have been described in the previous work.[11,22–26] Here, only a brief description is given. A schematic of the experimental setup is shown in Fig. 1. The system is operated in open air at atmospheric pressure. The gliding arc discharge is ignited at the narrowest gap between two diverging electrodes, made of hollow stainless steel tubes with an outer diameter of 3 mm and internally water-cooled. The minimum gap between the

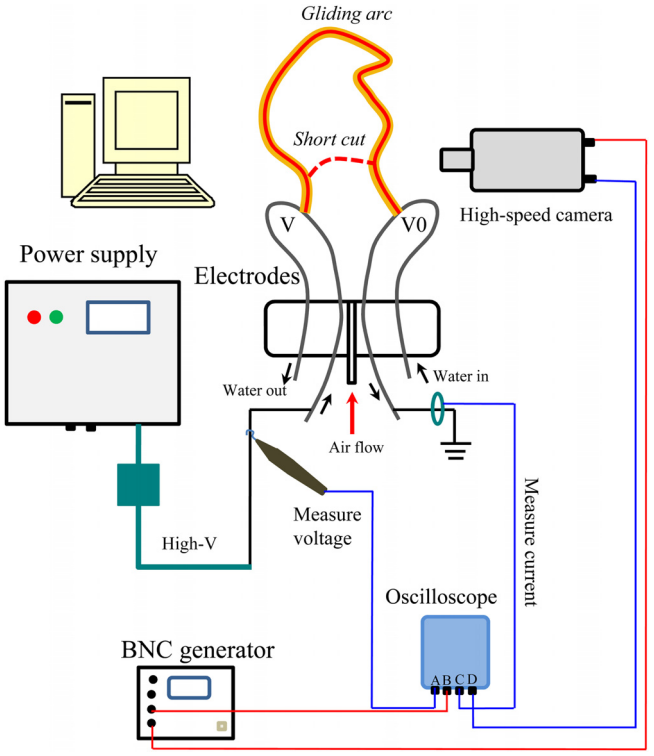

FIG. 1. A schematic of the experimental setup.

two electrodes is about 5 mm. One of the electrodes is connected to a 35 kHz AC power supply (Generator 9030 E, SOFTAL Electronic GmbH), whereas the other is grounded. The rated output power of this power supply can be manually adjusted with a minimal step of 50 W, but the current and voltage cannot be manually controlled. The air flow is ejected through a 3-mm diameter tube between the two electrodes to push the initial plasma column upward, forming the so-called gliding arc.

A current monitor (Pearson Electronics) and a voltage probe (Tektronix P6015A) are used to measure the waveforms of the current and the voltage simultaneously. A high-speed camera (HSC, Fastcam Photron SA-X2) equipped with an objective lens (Micro-Nikkor 105 mm, f/11) is synchronized to capture the dynamics of the gliding arc discharge. Measurements are performed at a frame rate of 50 kHz with an exposure time of 16.25 μs. The current and voltage signals together with the HSC gate and the external trigger signal are simultaneously recorded using a four-channel oscilloscope (PicoScope 4424, PS) at a sample rate of 2 GHz. The synchronization between the current/voltage and the HSC is realized through the external triggering using a pulse generator (BNC 575).

B. A current-voltage lumped model

To interpret the experimental results and obtain more detailed knowledge, modeling analysis is conducted. Here, a current (I)-voltage (U) lumped model is developed to analyze the I-U characteristics for obtaining more quantitative information about the gliding arc discharge. The following assumptions are made based upon experimental observations.

(1) The gliding arc is described as a plasma column with a small radius (r_{arc}), which is as an input parameter. The full width at half maximum (FWHM) of the radial intensity profile of the glow-type discharge is around 1 mm,[23] so the radius is set to 0.5 mm here.
(2) The input energy from the power supply is efficiently dissipated through the transfer of energetic molecules to cold ambience. The translational temperature of the plasma column is assumed to be stable.
(3) The electric field inside the plasma column is uniform and thus can be estimated by the measured voltage and the arc length (l_{arc}). The voltage drop in the cathode sheath (around 300 V) is relatively small compared with the measured input voltage.

The control volume in the model is the whole plasma column with a fixed radius [i.e., assumption (1)] and a varying length. The governing equation to describe the electric behavior mainly includes the electron conservation equation, as expressed by the following equation:

$$\frac{\mathrm{d}(\pi r_{arc}^2 l_{arc} n_e)}{\mathrm{d}t} = \pi r_{arc}^2 l_{arc}(R_e - R_{re}), \tag{1}$$

where l_{arc} is the length of the gliding arc, n_e is the average number density of free electrons in the plasma column, R_e represents the effective ionization rate in the plasma column, and R_{re} represents the effective recombination rate. As we know, the dominating ionization mechanism in the glow discharge is not well understood yet. There are mainly two kinds of ionization mechanism depending on the local environments: electron impact ionization and associative/Penning ionization.[27–30] Usually, the electron impact ionization is dependent on the reduced electric field (E/N, where E is the electric field strength and N is the molecular number density), while the associative ionization is independent of the reduced electric field. Benilov and Naidis[27] and Prevosto *et al.*[30] pointed out that the electron impact ionization can be replaced by associative ionization (e.g., $N + O \Rightarrow NO^+ + e$) at high-current glow discharges. Considering the relatively large discharge current here, the Arrhenius formula [Eq. (2)], which is widely used to express the radical reaction rate, is assumed to describe the effective rate of associative ionization in the plasma channel

$$R_e = \frac{n_e}{\tau_i} \exp\left(-\frac{E_a}{T_g R_u}\right), \tag{2}$$

where τ_i is a pre-exponential factor, E_a is the effective activation energy, R_u is the universal gas constant, and T_g is the gas temperature. The effective recombination rate is described by Eq. (3), which has been used to describe the recombination of NO^+ and the electron[28]

$$R_{re} = C_1 \frac{n_e^2}{T_e^{0.7}}, \tag{3}$$

where C_1 is a fitted parameter and T_e is the electron temperature with unit K. The electric current is calculated from n_e, using the following expression:

$$I = \pi r_{arc}^2 n_e e \mu_e E, \tag{4}$$

where e is the elementary charge and μ_e is the electron mobility, which can be estimated from the Bolsig+ simulation.[31]

The energy balance is important to understand the glow discharge. Considering the non-thermal properties, the translational temperature and the vibrational temperature are distinguished to investigate the energy dissipations, similar to Refs. 28, 30, and 32. The radial energy transport is written as

$$\rho c_p \frac{dT_g}{dt} - \frac{1}{r}\frac{d}{dr}\left[r\lambda\frac{dT_g}{dr}\right] = \eta_T J \times E + Q_{VT}, \tag{5}$$

$$\frac{n_{N_2} d\varepsilon_V}{dt} - \frac{1}{r}\frac{d}{dr}\left[r n_{N_2} D_{N_2}\frac{d\varepsilon_V}{dr}\right] = \eta_V J \times E - Q_{VT}, \tag{6}$$

where ρ is the gas density, c_p is the heat capacity at constant gas pressure, T_g is the gas temperature, λ is the gas thermal conductivity, η_T represents the fraction of Joule energy that goes to the translational degrees of freedom, J is the current density, ε_v is the mean vibrational energy of nitrogen molecules, D_{N2} is the diffusion coefficient of N_2 molecules, n_{N2} is the number density of N_2, η_V represents the fraction of Joule energy that goes to the vibrational excitation of N_2, and Q_{VT} is the vibrational-to-translational (V-T) relaxation rate of N_2 molecules, which can be modeled through the term below

$$Q_{VT} = n_{N_2}\frac{\varepsilon_V - \varepsilon_V(T_g)}{\tau_{VT}}, \tag{7}$$

where τ_{VT} is the relaxation time, which is expressed as[33]

$$\tau_{VT} = 6.5 \times 10^{-4} \exp\left(\frac{137}{T_g^{1/3}}\right)/P[\text{Pa}], \tag{8}$$

$\varepsilon_v(T_g)$ is the equilibrium mean vibration energy at gas temperature, which is given by

$$\varepsilon_V(T_g) = \frac{E_{N_2}}{\exp(E_{N_2}/T_g) - 1}, \tag{9}$$

where E_{N2} is the vibrational excitation level of N_2 (0.29 eV). During the energy transport simulation, the fluxes at the boundaries are set to zero. The initial temperature is assumed to follow the Gaussian profile.

Shortly, in the model, the input parameters include input voltage, arc length, and radius, which can be directly derived from the experiments. The output parameters include current, electron density, and radial temperature profiles. Undetermined parameters of the model are fitted by comparing the current value from simulation to the experiments.

III. RESULTS AND DISCUSSION

A. Characteristics of a sustained glow-mode gliding arc

Figure 2(a) shows a typical voltage and current waveform of the gliding arc at a time span of 0.95 s with a flow rate of 7 l/min. The detailed voltage and current waveforms are close to a sinusoidal shape, as illustrated in Fig. 2(b).

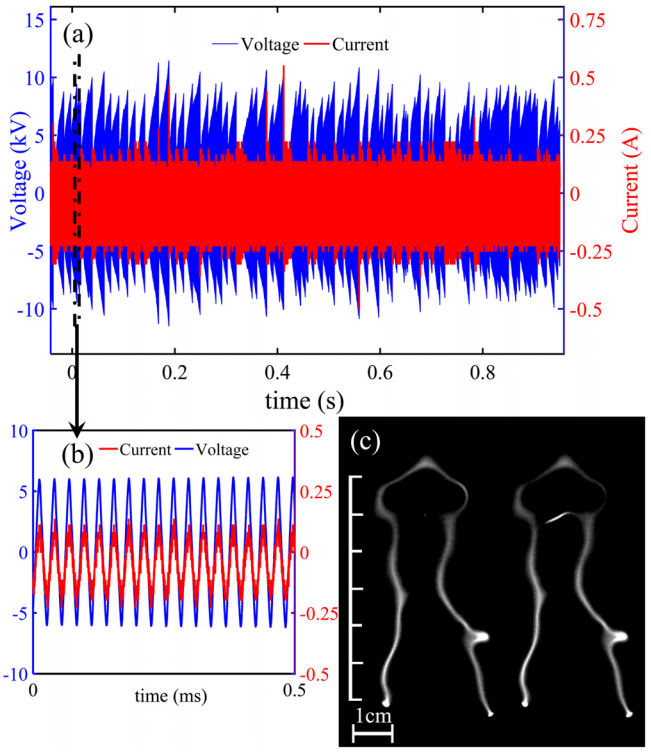

FIG. 2. (a) Typical voltage and current waveforms of the gliding arc at a flow rate of 7 l/min. (b) Detailed voltage and current waveforms within a time span of 0.5 ms. (c) Images of the gliding arc acquired using a high-speed camera (16.25 μs exposure time).

After the breakdown of the air flow at the smallest gap between the electrodes, the gliding arc is sustained without re-ignition for a relatively long time (more than several seconds). Both the recorded voltage and current waveforms show a sawtooth-like envelope. The peak voltage varies from about 4 kV to 12 kV, and the current is mostly below 0.5 A, without current spikes larger than 1 A. At the atmospheric pressure, the plasma is easily contracted into the filament, as shown in Fig. 2(c). However, it does not belong to an arc since the current is quite small and the gas temperature is not very high (<3000 K). The cathode current density is estimated to be on the same order of 4.4 A/cm^2 according to the current and the cathode spot size.[11] The cathode fall here cannot be experimentally measured in the current setup, but a pin-to-pin setup using the same power supply was tested to estimate the cathode fall, which reached 460 V. Therefore, we suppose that the GA discharge has a similar cathode fall. Similar plasma columns have been detected and called as glow discharge in the literature.[29,30,34] The detected discharge here can also be regarded as a glow-mode gliding arc although it is not as diffusive as that in the low-pressure glow discharge.

The instantaneous length of the plasma column is derived from the high-speed images, using a binarization method and the "regionprops" function in the Matlab software. The probed voltage is divided by the plasma length to give the mean electric field strength (E), as shown in Fig. 3. Although the voltage envelope varies from 3 kV to 12 kV (see Fig. 2), the variation of the electric field strength envelope is relatively small with a mean value of 65 kV/m. It

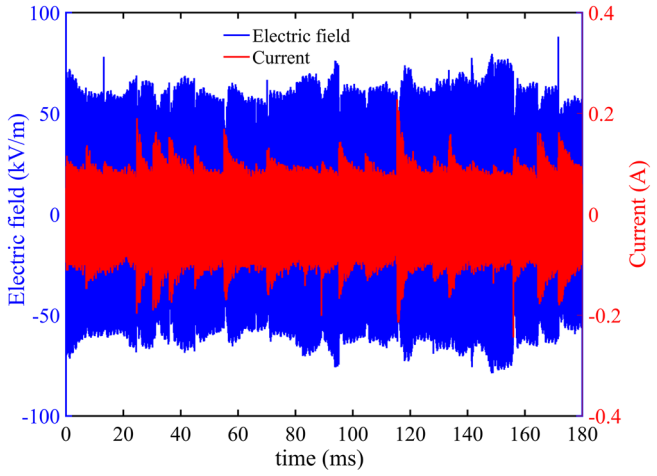

FIG. 3. Electric field strength and current waveforms of the gliding arc at a flow rate of 7 l/min.

should, however, be mentioned that 3D-effects were not considered when the length of the gliding arc was estimated. Disregarding the third dimension could cause underestimations of the arc length,[24] and thus, the electric field strength is overestimated a little. The current envelope is sawtooth-like due to the short-cutting events of plasma columns, which is also termed as "back breakdown" in Refs. 17 and 35. During every short-cutting event, the current can rise up fast and then decay to a specific value before the next short-cutting event.

The gas temperature of a sustained diffusive gliding arc discharge has been estimated to about 1600 K using the empirical formula presented by Zhu *et al.*[11] The gas temperature of a glow-type gliding arc discharge with an input power of 800 W and an air flow of 17.5 l/min is around 1110 K that was measured by the Rayleigh scattering method.[25] Thus, the reduced electric field strength is around 9 Td calculated by using the measured electric field strength and the temperature of the plasma column. The corresponding mean electron temperature is estimated to be 0.9 eV using the BOLSIG+ Boltzmann solver.[31] During the BOLSIG+ simulation, the cross sections for N_2 and O_2 are from the SIGLO database and the Phelps database in LXCat, respectively.[36] The volumetric ratio between N_2 and O_2 is set to 4:1.

In general, with a slow jet flow, the glow-mode gliding arc discharge can be maintained in a time scale of seconds without extinction. The translational temperature is between 1000 K and 2000 K. The mean reduced electric field is below 15 Td, and the average electron energy is around 1 eV. These discharge properties are similar to the magnetically stabilized gliding arc discharge (MSGAD).[21] Table I lists the properties of some typical discharges. The glow-mode gliding arc has a relatively higher current and a lower electric field strength.

B. Dynamical behavior of electron density inside the plasma column

In the experiment, no phase shift between the current waveforms and the voltage waveforms is detected during the glow-mode discharge, so the plasma column can be treated as a pure resistance. The electron number density, which is thus derived from the peak current and voltage during every period of the power supply, is shown in Fig. 4. The variation of electron density in the detected time span is confirmed. During every short cutting event, the electron density rises up and then decays slowly, tending to a value of around $2.5 \times 10^{19}\,m^{-3}$ within a timescale of milliseconds. However, before reaching the stable state, the short cutting event occurs and thus the electron density rises up again. Therefore, the electron density is largely above the stable state for the GM-GA discharge here. Maybe if the short-cutting events are controlled, the electron number density can be sustained at around $2.5 \times 10^{19}\,m^{-3}$.

The decaying rate has been fitted with the effective model [see Eq. (1)] in Fig. 4. During fitting, the gas temperature is assumed to be constant (~1500 K). It means that the rate is solely dependent on the electron density and the electron temperature. The fitted result is not perfect, but the tendency is well predicted. The effective ionization time and recombination time are as long as 5.5 ms and 4.8 ms, respectively. It implies that at this stage, the effective ionization and recombination are both slow and not as violent as that during electrical breakdown. Although the glow-mode GA discharge is not in a steady state from a time scale of milliseconds, the electron density can be treated as a quasi-steady state within the time scale of tens of microseconds if necessary.

Here, the short-cutting events play an important role to keep the glow-mode GA discharge. It not only recovers the electron density but also limits the maximum length of the plasma column. As plotted in Fig. 5, the short-cutting events confine the continuous growing of the gliding arc and result in the sawtooth-like curve of the arc length. In the flow, the gliding arc needs to elongate to follow the flowing gas and thus dissipates more energy. Since the input power is limited, the length of the plasma column could not increase infinitely. For the conventional gliding arc, the length of the arc channel is confined mainly due to the reignition at the smallest

TABLE I. Comparison between discharge properties.

Parameter	GM-GA	MSGAD[21]	Glow discharge[37,38]	Thermal arc[39]
Current (mA)	100–500	30–200	0.4–10	>10 000
Electric field (V/cm)	400–900	200–800	1400–5000	20–100
E/N parameter (Td)	5–15	5–25	30–50	0.5–2
Gas temperature (K)	1000–2000	2200–2500	300–1550	>10 000
Average electron energy (eV)	0.8–1	0.8–1.1	1.2–1.4	1–5
Cathode current density (A/cm^2)	~4.4[11]	4.5–8.2	~5.8	10^4–10^7
Electron density (cm^{-3})	~10^{13}	(0.1–3) × 10^{14}	~10^{13}	10^{16}–10^{19}

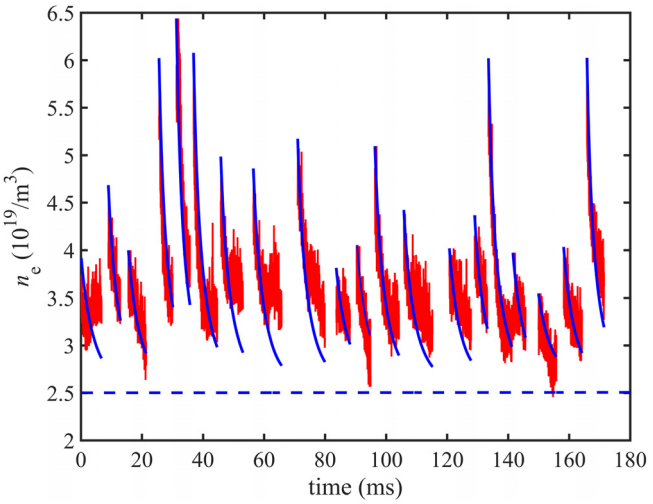

FIG. 4. Electron number density variation with time, together with the fitted values (blue curves). During fitting, $C_1 = 3.4 \times 10^{-15}$, $E_a = 16628$, and $\tau_i = 1.45 \times 10^{-3}$.

gap of two electrodes.[20] However, for the glow-mode gliding arc discharge here, the short cutting event becomes the main approach to limit the arc length. Therefore, the GM-GA discharge can stay in the non-thermal state without reignition for a long time. It is noted that the short-cutting events occur due to the twisting, stretching, and wrinkling of the plasma column. A longer plasma column will promote the occurrence of short cutting events. An increase in the gap width between electrodes can increase the re-ignition voltage, thus resulting in a longer plasma column and more short cutting events. The gap distance between electrodes here is 5 mm, larger than the common value (2–3 mm). This may contribute to the special GM-GA discharge. On the other hand, the turbulent flow, which stretches and wrinkles the plasma column, can make a large difference as well.

C. Energy dissipation in the GM-GA discharge

In order to analyze the energy dissipation around the plasma column, the translational temperature (T_g) and the vibrational temperature of N_2 (T_v) are simulated with an input power density determined from measured current and electric field strength. The input power density is assumed to follow a Gaussian profile with a variance of 0.5 mm. Usually, more than 98%[40] of the input electric power is first transferred to the vibrational excitation of N_2. Later, the gas is heated due to the vibrational-translational (V-T) transition. Using a presumed initial temperature profile and the experimental power density, the variations of peaks T_g and T_v, together with the typical temperature profiles, are illustrated in Fig. 6. With η_V and η_T equal to 0.98 and 0.02, respectively, the peak T_v can be stabilized at around 6000 K and the peak T_g is around 3000 K. The ratio of peaks T_v and T_g (T_v/T_g) is close to 2. This large difference between vibrational and translational temperatures appears in the center part of the plasma column, but outside the plasma column, the difference becomes much smaller, as illustrated in Fig. 6(c). It is mainly attributed to the large input power density in the plasma core and the strong energy dissipations by cold surroundings.

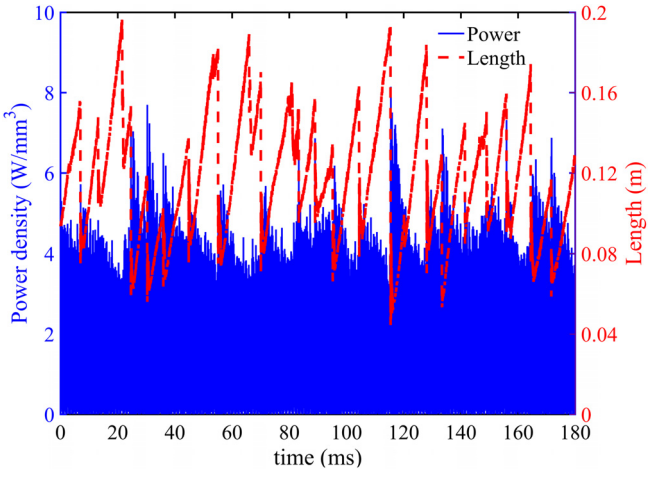

FIG. 5. Input electrical power density together with the plasma column length.

For the GM-GA discharge here, the vibrational temperature of NO has been estimated from the emission spectra,[25] which is around 5900 K, close to the simulated value. However, the measured translational temperature is much lower than the simulated value with η_V being equal to 0.98. In order to reduce T_g, η_v is decreased to 0.48 in the model. Then, the peak T_v becomes around 5000 K and the peak T_g remains around 2000 K, as shown in Fig. 6(b). Although the Rayleigh measurement may have large error bars, we prefer to believe that the gas temperature is still far below 3000 K but near 2000 K. If this is true, other pathways should exist to dissipate the energy since η_v is only 0.48. According to the images, the glow-mode plasma column looks partially diffusive. Furthermore, the emission spectra have been measured to indicate various active radical species (e.g., NO, OH, NH, N_2, and O).[25] Therefore, some endothermic reactions are speculated to occur in the glow discharge to dissipate the energy.

D. Discussion of the chemical states in the glow-mode GA discharge

The chemical compositions of the plasma column can be related to the ionization/recombination rates and the energy dissipation. However, the detailed compositions are not easy to determine. Here, the chemical equilibrium compositions are simulated using the chemical equilibrium program CEA[41] to estimate the chemical composition of the plasma column. The chemical equilibrium compositions of the gaseous mixture (O_2:N_2:H_2O = 21:78:1 by volume) at different temperatures are calculated and listed in Table II. It is found that the electron density close to our measurements can be reached at around 4500 K and the positive ion is largely NO^+. Oxygen molecules are mostly decomposed to atomic oxygen above 4000 K. Although the glow-mode GA discharge here is certainly non-equilibrium, the assumption is still made that the glow-mode plasma has a similar chemical composition to the equilibrium state at 4500 K but has a much lower gas temperature due to the strong heat

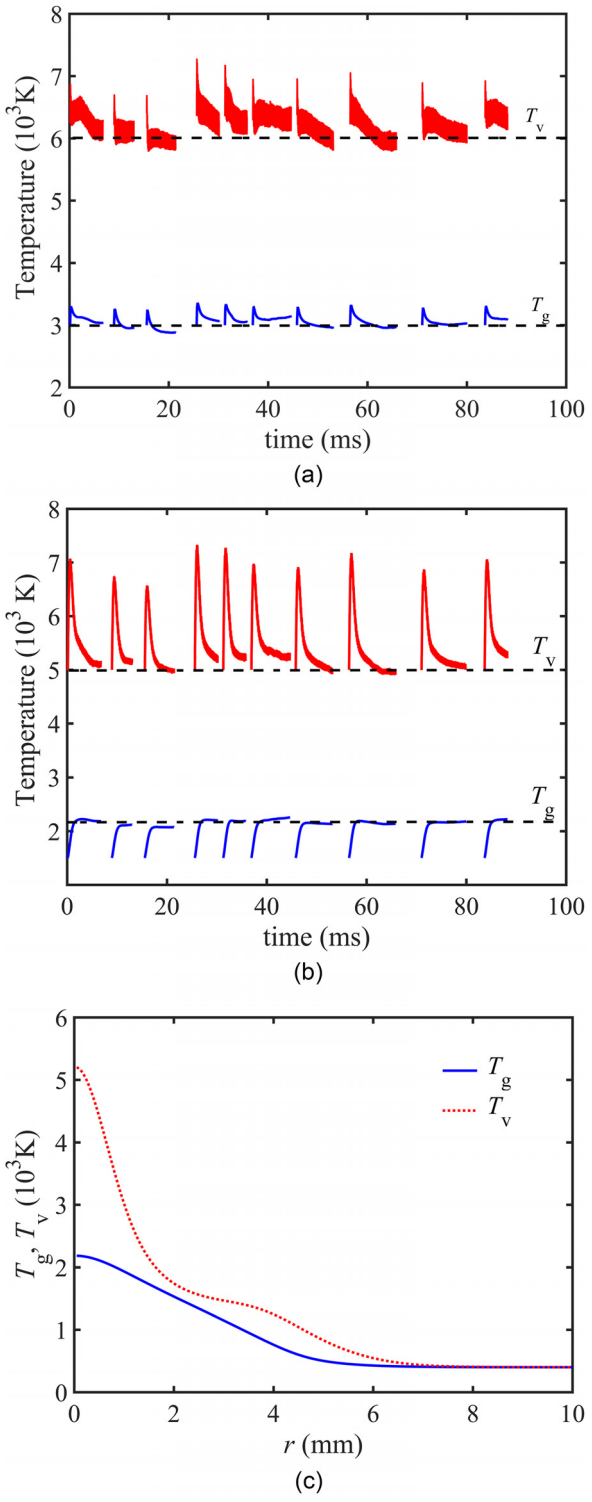

FIG. 6. Variations of the peak gas temperature and vibrational temperature with time. (a) $\eta_V = 0.98$ and (b) $\eta_V = 0.48$. (c) The typical temperature profiles of T_g and T_v.

dissipation. In fact, considering the high vibrational temperature and the electron temperature, the chemical composition of a 2000 K gas is very likely to be as decomposed as that at a temperature of 4500 K.

Based upon this assumption, both the slow effective ionization/recombination processes and the energy dissipation can be reasonably explained. Because the electron density is close to the equilibrium state, the ionization and the recombination are relatively slow and insensitive to E/N. The chemical or associative ionizations should be dominating in this hot gaseous mixture. Since the oxygen molecule has been largely decomposed into oxygen atoms, an energy sink term [see Eq. (10)] can be estimated due to the endothermic reaction (i.e., $O_2 = 2O$)

$$Q_{dis} = \Delta H \times n_{O2}/\tau_O, \tag{10}$$

where τ_O is the residence time in the plasma column due to the diffusion or convection, ΔH is the reaction enthalpy, and n_{O2} is the density of oxygen molecules. For a residence time of 3 ms, Q_{dis} can be as high as 10^9 W/m^3. This rough estimation indicates the potentially large impacts of endothermic reactions and mass transports of active radicals.

E. Short discussion of sustaining a glow-mode discharge

To maintain a stable glow-mode discharge, the plasma temperature and the electron density must be restrained in a reasonable range. It requires the source terms on the right side of Eq. (1) not to be positive since a positive electron source can trigger the thermal instability of atmospheric discharge easily. There are two types of ionizations: associative ionization and electron impact ionization. The electron impact ionization (including the stepwise ionization) is sensitive to the averaged electric field (E_{ave}) which is the voltage divided by the arc length, while the associative ionization is insensitive to E_{ave}. Therefore, when the associative ionization governs the electron production, the fluctuation of E_{ave} could not make the source terms positive, and thus, the discharge is stable. Nevertheless, if the electron impact ionization becomes comparable to the associative ionization, the glow-type discharge will become instable and transit to spark discharges due to E_{ave} fluctuations.

The reduced electric field (E/N), which is a combination of the electric field strength (E) and the temperature profiles, is a crucial parameter to control the volumetric ionization. In order to prevent the electron impact ionization governing the electron production, the temperature and E should be well confined. The temperature profile in the plasma column is governed by the energy equation which is affected by the flow field (i.e., convection). Manipulating the flow field is one way to sustain the glow-type discharge. The electric field strength depends on the voltage drop over the electrodes. For the power supply used in this study, the rated power, rather than the voltage, is manually set during operation. Hence, the voltage will drop automatically when the current is high during sparks to constrain the further thermalization of the plasma column. In the discharge systems used by Machala *et al.*[34] and Staack *et al.*,[42] a ballast resistor was applied to stabilize the glow discharge. This ballast resistor has similar effects to the power supply used here that it limits the voltage when the current increases. This kind of feedback from the power system is necessary to control the glow-to-spark transition in the atmosphere.

TABLE II. Mole fractions (x) of species in the hot gas mixture.

T_g (K)	2500	3000	3500	4000	4500	5000
x_e	4.17×10^{-10}	2.57×10^{-8}	4.47×10^{-7}	3.27×10^{-6}	1.38×10^{-5}	4.20×10^{-5}
x_H	2.53×10^{-4}	2.95×10^{-3}	9.47×10^{-3}	1.42×10^{-2}	1.58×10^{-2}	1.61×10^{-2}
x_{H2O}	7.62×10^{-3}	3.17×10^{-3}	4.22×10^{-4}	2.56×10^{-5}	1.46×10^{-6}	1.16×10^{-7}
x_N	2.54×10^{-7}	1.19×10^{-5}	1.83×10^{-4}	1.42×10^{-3}	7.08×10^{-3}	2.57×10^{-2}
x_{NO}	2.18×10^{-2}	4.04×10^{-2}	5.00×10^{-2}	4.14×10^{-2}	2.77×10^{-2}	1.82×10^{-2}
x_{NO+}	4.43×10^{-10}	2.67×10^{-8}	4.60×10^{-7}	3.33×10^{-6}	1.39×10^{-5}	4.21×10^{-5}
x_{N2}	7.65×10^{-1}	7.38×10^{-1}	6.89×10^{-1}	6.47×10^{-1}	6.29×10^{-1}	6.11×10^{-1}
x_O	6.34×10^{-3}	4.50×10^{-2}	1.49×10^{-1}	2.62×10^{-1}	3.12×10^{-1}	3.26×10^{-1}
x_{OH}	4.31×10^{-3}	9.55×10^{-3}	7.58×10^{-3}	2.81×10^{-3}	8.06×10^{-4}	2.51×10^{-4}
x_{O2}	1.94×10^{-1}	1.60×10^{-1}	9.33×10^{-2}	3.14×10^{-2}	7.98×10^{-3}	2.20×10^{-3}

IV. CONCLUSION

This article aims at gaining a better understanding of the glow-mode gliding arc (GM-GA) generated in atmospheric air. The electron conservation and the energy balance of the GM-GA discharge are considered to build a current-voltage lumped model for analyzation of the discharge characteristics, dynamical behavior of electron density, and energy dissipations.

The electron number density in the GM-GA discharge reaches as high as $3 \times 10^{19}\,m^{-3}$ and is always above the steady value due to the short cutting events, which can recover the electron density to a relatively large value and limits the maximum length of gliding arc. The fitted effective ionization and recombination time are as long as 5.5 ms and 4.8 ms, respectively. These slow ionization and recombination processes are possibly attributed to the near-equilibrium chemical compositions in the active plasma column.

Due to the huge input power density and the violate energy dissipation, the plasma is non-thermal with T_v/T_g larger than 2. Energy is mainly dissipated through mass transports of vibrationally excited nitrogen and active radicals.

ACKNOWLEDGMENTS

This work was financially supported by the Swedish Energy Agency, the Swedish Research Council, the Knut and Alice Wallenberg foundation, the European Research Council, and the National Natural Science Foundation of China (No. 51606217).

[1]S. P. Gangoli, A. F. Gutsol, and A. Fridman, Plasma Sources Sci. Technol. **19**, 065003 (2010).
[2]T. Ombrello, Y. Ju, and A. Fridman, AIAA J. **46**, 2424–2433 (2008).
[3]T. Ombrello, X. Qin, Y. Ju, A. Gutsol, A. Fridman, and C. Carter, AIAA J. **44**, 142–150 (2006).
[4]Y. Kusano, S. Teodoru, F. Leipold, T. L. Andersen, B. F. Sørensen, N. Rozlosnik, and P. K. Michelsen, Surf. Coat. Technol. **202**, 5579–5582 (2008).
[5]Y. Kusano, B. F. Sorensen, T. L. Andersen, H. L. Toftegaard, F. Leipold, M. Salewski, Z. Sun, J. Zhu, Z. Li, and M. Alden, J. Phys. D: Appl. Phys. **46**, 135203 (2013).
[6]Y. Kusano, J. Adhes. **90**, 755–777 (2014).
[7]C. Du, J. Yan, X. Li, B. Cheron, X. You, Y. Chi, M. Ni, and K. Cen, Plasma Chem. Plasma Process. **26**, 517–525 (2006).
[8]M. Gallagher, R. Geiger, A. Polevich, A. Rabinovich, A. Gutsol, and A. Fridman, Fuel **89**, 1187–1192 (2010).
[9]V. Dalaine, J. Cormier, S. Pellerin, and P. Lefaucheux, Appl. Phys. **84**, 1215–1221 (1998).
[10]C. Kalra, A. Gutsol, and A. Fridman, IEEE Trans. Plasma Sci. **33**, 32–41 (2005).
[11]J. Zhu, J. Gao, Z. Li, A. Ehn, M. Alden, A. Larsson, and Y. Kusano, Appl. Phys. Lett. **105**, 234102 (2014).
[12]S. Lu, X. Sun, X. Li, J. Yan, and C. Du, Phys. Plasmas **19**, 072122 (2012).
[13]L. Yu, J. Yan, M. Ni, Y. Chi, X. Li, and S. Lu, IEEE Trans. Plasma Sci. **39**, 2832 (2011).
[14]Y. D. Korolev, O. B. Frants, N. V. Landl, A. V. Bolotov, and V. O. Nekhoroshev, Plasma Sources Sci. Technol. **23**, 054016 (2014).
[15]S. Kolev and A. Bogaerts, Plasma Sources Sci. Technol. **24**, 065023 (2015).
[16]S. Kolev and A. Bogaerts, Plasma Sources Sci. Technol. **24**, 015025 (2015).
[17]S. Sun, S. Kolev, H. Wang, and A. Bogaerts, Plasma Sources Sci. Technol. **26**, 015003 (2017).
[18]S. Sun, S. Kolev, H. Wang, and A. Bogaerts, Plasma Sources Sci. Technol. **26**, 055017 (2017).
[19]A. Fridman, A. Chirokov, and A. Gutsol, J. Phys. D: Appl. Phys. **38**, R1–R24 (2005).
[20]A. Fridman, S. Nester, L. A. Kennedy, A. Saveliev, and O. Mutaf-Yardimci, Prog. Energy Combust. **25**, 211–231 (1999).
[21]S. Gangoli, A. Gutsol, and A. Fridman, Plasma Sources Sci. Technol. **19**, 065004–065007 (2010).
[22]Z. Sun, J. Zhu, Z. Li, M. Alden, F. Leipold, M. Salewski, and Y. Kusano, Opt. Express **21**, 6028–6044 (2013).
[23]J. Zhu, Z. Sun, Z. Li, A. Ehn, M. Alden, M. Salewski, F. Leipold, and Y. Kusano, J. Phys. D: Appl. Phys. **47**, 295203–295211 (2014).
[24]J. Zhu, J. Gao, A. Ehn, M. Alden, Z. Li, D. Moseev, Y. Kusano, M. Salewski, A. Alpers, P. Gritzmann, and M. Schwenk, Appl. Phys. Lett. **106**, 044101 (2015).
[25]J. Zhu, "Optical diagnostics of non-thermal plasmas and plasma-assisted combustion," Ph.D. thesis, Lund University (Lund Reports on Combustion Physics, LRCP-188, 2015).
[26]J. Zhu, J. Gao, A. Ehn, M. Alden, A. Larsson, Y. Kusano, and Z. Li, Phys. Plasmas **24**, 013514 (2017).
[27]M. Benilov and G. Naidis, J. Phys. D: Appl. Phys. **36**, 1834–1841 (2003).
[28]L. Yu, C. Laux, D. Packan, and C. Kruger, J. Appl. Phys. **91**, 2678 (2002).
[29]M. Xaubet, L. Giuliani, D. Grondona, and F. Minotti, Phys. Plasmas **24**, 013502 (2017).
[30]L. Prevosto, H. Kelly, B. Mancinelli, J. C. Chamorro, and E. Cejas, Phys. Plasmas **22**, 023504 (2015).
[31]G. Hagelaar and L. Pitchford, Plasma Sources Sci. Technol. **14**, 722–733 (2005).
[32]N. A. Popov, Plasma Phys. Rep. **32**, 237–245 (2006).
[33]J. A. Riousset, V. P. Pasko, and A. Bourdon, J. Geophys. Res. **115**, A12321, doi:10.1029/2010JA015918 (2010).
[34]Z. Machala, E. Marode, C. O. Laux, and C. H. Kruger, J. Adv. Oxid. Technol. **7**, 133–137 (2004).
[35]S. Pellerin, O. Martinie, J. M. Cormier, J. Chapelle, and P. Lefaucheux, High Temp. Mater. Processes **2**, 167–180 (1999).
[36]L. C. Pitchford, L. L. Alves, K. Bartschat, S. F. Biagi, M.-C. Bordage, I. Bray, C. E. Brion, M. J. Brunger, L. Campbell, A. Chachereau *et al.*, Plasma Processes Polym. **14**, 1600098 (2017).

[37]D. Staack, B. Farouk, A. Gutsol, and A. Fridman, Plasma Sources Sci. Technol. **14**, 700 (2005).
[38]D. Staack, B. Farouk, A. Gutsol, and A. Fridman, Plasma Sources Sci. Technol. **15**, 818 (2006).
[39]A. Fridman and L. Kennedy, *Plasma Physics and Engineering* (Taylor and Francis, London, UK, 2004).
[40]N. A. Popov, Plasma Phys. Rep. **27**, 886–896 (2001).
[41]S. Gordon and B. J. McBride, "Computer program for calculation of complex chemical equilibrium compositions and applications," NASA Reference Publication No. 1311 (1996).
[42]D. Staack, B. Farouk, A. Gutsol, and A. Fridman, Plasma Sources Sci. Technol. **17**, 025013 (2008).